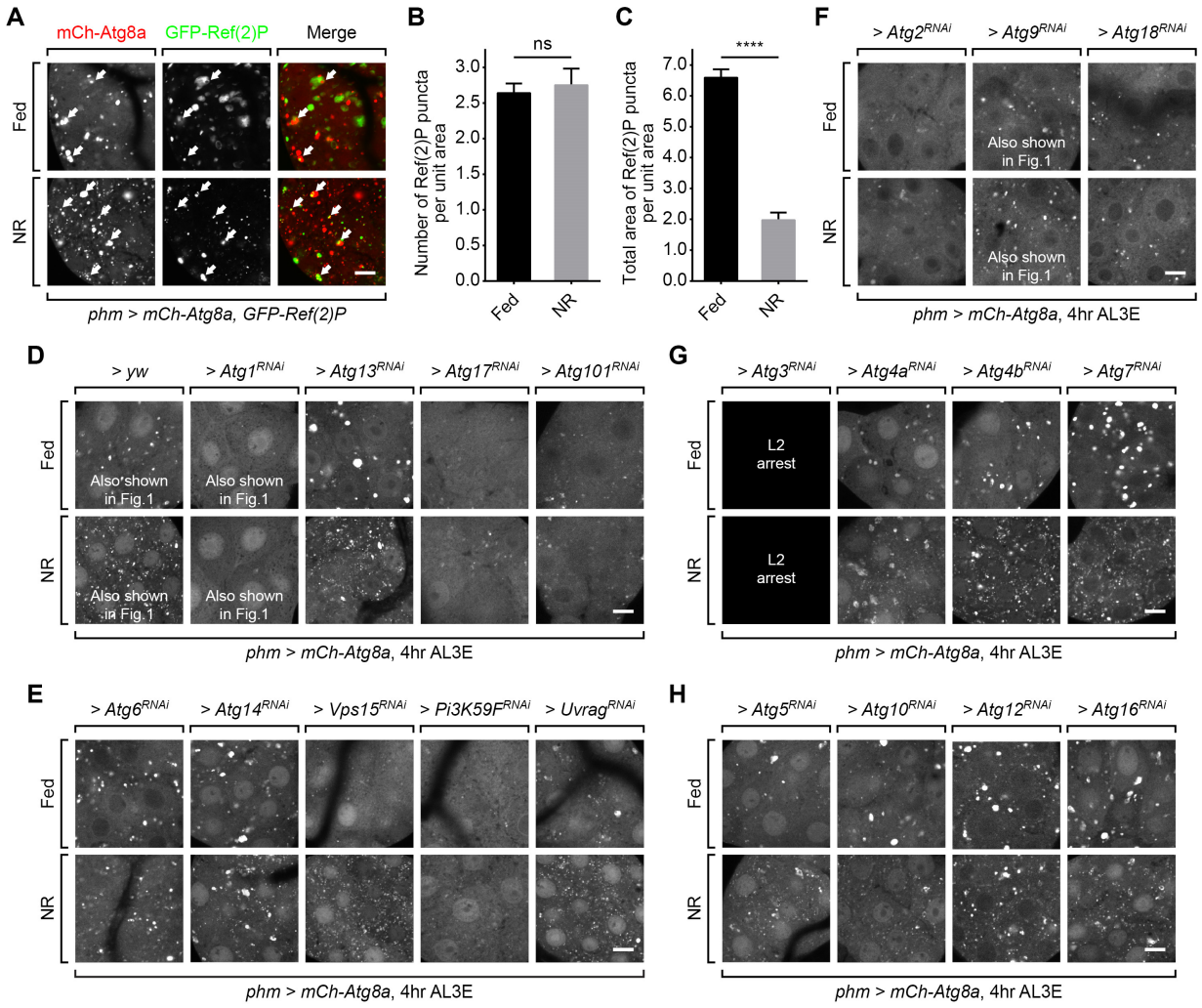

Figure S1. Autophagy in the PG is controlled by a subset of *Atg* genes and the upstream TOR pathway. Related to Figure 1.

(A) Protein aggregates and autophagosomes visualized by GFP-Ref(2)P and mCh-Atg8a respectively in fed and starved pre-NRC (4 hrs AL3E) larvae. Arrows indicate the colocalization between Ref(2)P- and Atg8a-positive structures. (B and C) Quantification of the number (B) and the total area (C) of Ref(2)P-positive structures per unit cell area (100 μm^2) in the PGs of fed and starved larvae. Mean ± SEM; p values by unpaired t-test (n=6 in fed group and n=8 in NR group; ns, not significant, ****p<0.0001). (D-H) Autophagic structures visualized by mCh-Atg8a in pre-NRC (4 hrs AL3E) larval PG tissues after single *Atg* gene knockdown. The majority of known Drosophila *Atg* genes were tested in five groups: the initiation complex that responds to TOR signaling (*Atg1*, *Atg13*, *Atg17* and *Atg101*) (D), the lipid kinase complex that mediates autophagosome formation (*Atg6*, *Atg14*, *Vps15*, *Pi3K59F* and *Uvrag*) (E), the Atg9 centered system whose function is not fully understood (*Atg2*, *Atg9* and *Atg18*) (F) and two ubiquitin-like conjugation systems for Atg5-Atg12-Atg16 complex (*Atg5*, *Atg10*, *Atg12* and *Atg16*) and Atg8-

PE formation (*Atg3*, *Atg4a*, *Atg4b* and *Atg7*) (G and H). Images of *phm>yw*, *phm>Atg1*^{RNAi} (D) and *phm>Atg9*^{RNAi} (F) samples are also shown in Figure 1E. (D-H) Scale bar, 10 μm.

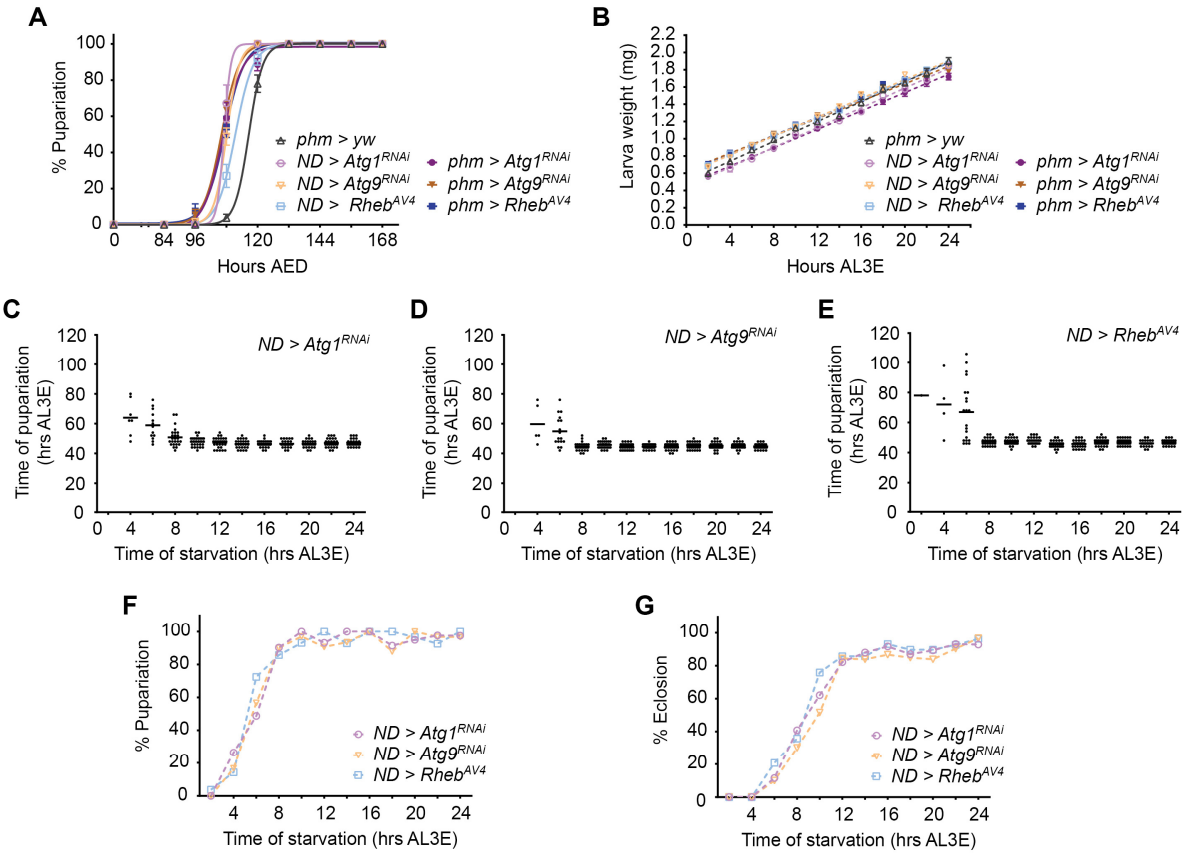

Figure S2. Autophagy suppression in the PG causes inappropriate pupariation during early stage NR. Related to Figure 2.

(A and B) Pupariation timing curve (A) and growth rate (B) of control (*phm-Gal4* and no driver (ND) control) and autophagy suppression larvae. (C-E) Relationship between start time of starvation and time from the L2/L3 molt to pupariation in *ND>Atg1^{RNAi}* (C), *ND>Atg9^{RNAi}* (D) and *ND>Rheb^{AV4}* (E) larvae (n>30 for each time point). (F and G) Percentage of larvae that manage to pupariate (F) and that eclose from pupa (G) after starvation treatment starting from different time points AL3E.

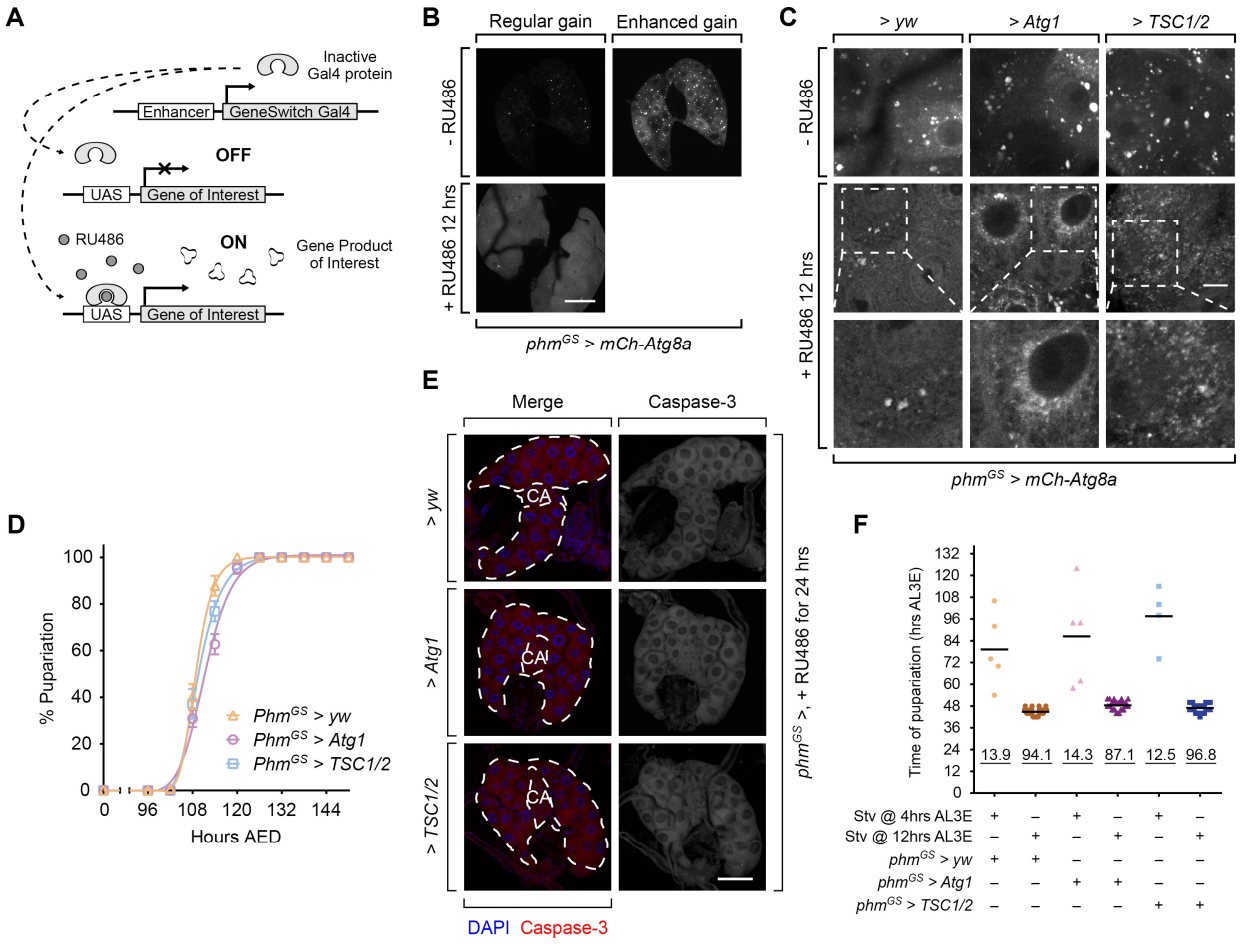

Figure S3. Forced autophagy induction in the PG causes developmental delay/arrest in fed larvae. Related to Figure 3.

(A) Schematic diagram showing the RU486-induced GeneSwitch system. (B) Expression of mCh-Atg8a in *phm^{GS}>mCh-Atg8a* PGs before and after RU486 treatment. RU486 treatment started at 12 hrs AL3E and lasted for 12 hrs. Both groups were imaged first under the same parameter (regular gain) to compare the level of target gene (here mCh-Atg8a) expression before and after RU486 treatment. Then the -RU486 image, whose fluorescence signal was almost indiscernible under regular gain, were retaken with enhanced gain to show the tissue outline. Scale bar, 50 μm. (C) Autophagy induction in the PG before and after RU486 induction in *phm^{GS}>yw*, *phm^{GS}>Atg1* and *phm^{GS}>TSC1/2* larvae at 12 hrs AL3E. In RU486 fed *phm^{GS}>Atg1* larvae the autophagic vesicles located at perinucleus region, which is consistent with previous study [S1], while in *phm^{GS}>TSC1/2* larvae these vesicles showed similar distribution as NR-induced autophagy (Figure 1B). Scale bar, 10 μm. (D) Pupariation timing curves of *phm^{GS}>yw*, *phm^{GS}>Atg1* and *phm^{GS}>TSC1/2* larvae without RU486 feeding. (E)

Immunofluorescence images of PGs in RU486 treated *phm^{GS}>yw*, *phm^{GS}>Atg1* and *phm^{GS}>TSC1/2* larvae. Larvae were fed with RU486 for 24 hrs, starting at 12 hrs AL3E, before dissection. PG tissues were then immunostained by antibody targeting cleaved caspase-3. Dash lines indicate the outline of PGs. Corpora allata (CA), whose cells were not affected by autophagy induction, were marked as internal controls. Scale bar, 50 μm. (F) Pupariation of larvae after starvation treatment starting at early L3 (4 hrs AL3E) or mid L3 (12 hrs AL3E) stage. The result confirmed that the NRCs for all the tested groups were achieved between 4 hrs and 12 hrs AL3E. The scattered dots indicate the time of pupariation of each individual larva. The underscored numbers indicate the rate of pupariation. For each group n > 30.

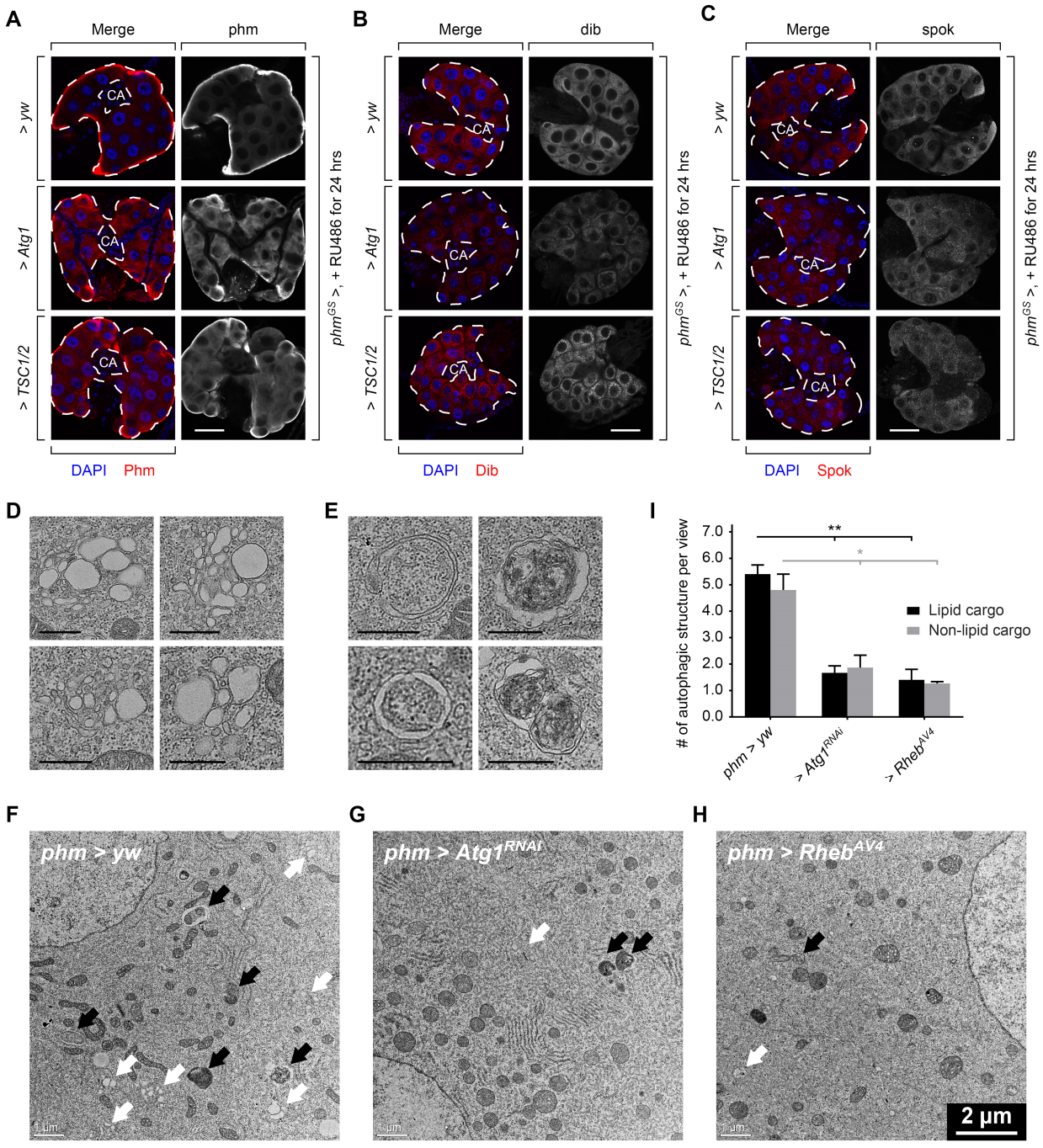

Figure S4. Autophagy blocks ecdysone synthesis by limiting cholesterol availability in PG cells. Related to Figure 4 and Figure 5.

(A-C) Immunofluorescence images of PGs in *phm*^{GS}*>yw*, *phm*^{GS}*>Atg1* and *phm*^{GS}*>TSC1/2* larvae. Larvae were treated with RU486 starting at 12 hrs AL3E and samples were dissected at 36 hrs AL3E. PG tissues were then immunostained with anti-Phm (A), anti-Dib (B) and anti-Spok

(C) antibodies. Dash lines indicate the outline of PGs. Corpora allata (CA), which do not express any Halloween gene, are also outlined and indicated in the images. Scale bar, 50 μm. (D) TEM images of lipophagy related structures which contain a cluster of small membrane bound vesicles with light-density contents. Scale bars, 0.5 μm. (E) TEM images of autophagic structures that contain non-lipid cargoes. Upper left, an early stage isolation membrane; lower left, a typical double membrane bound autophagic vesicle; upper and lower right, late-stage autophagic structures with condensed cytoplasmic material. Scale bar, 0.5 μm. (F-H) Low magnification (4700x) TEM images of PG cells of starved *phm>yw* (F), fed *phm>Atg1*^{RNAi} (G) and fed *phm>Rheb*^{AV4} (H) larvae. Autophagic structures that contain lipid and non-lipid contents are annotated by white and black arrows respectively. (I) Quantification of the number of autophagic structures in a single view under low magnification TEM (4700x). For each biological sample, 5 random images were taken and the autophagic structures were identified and counted manually. Mean ± SEM; p values by unpaired t-test (n=3; *p<0.05, **p<0.01).

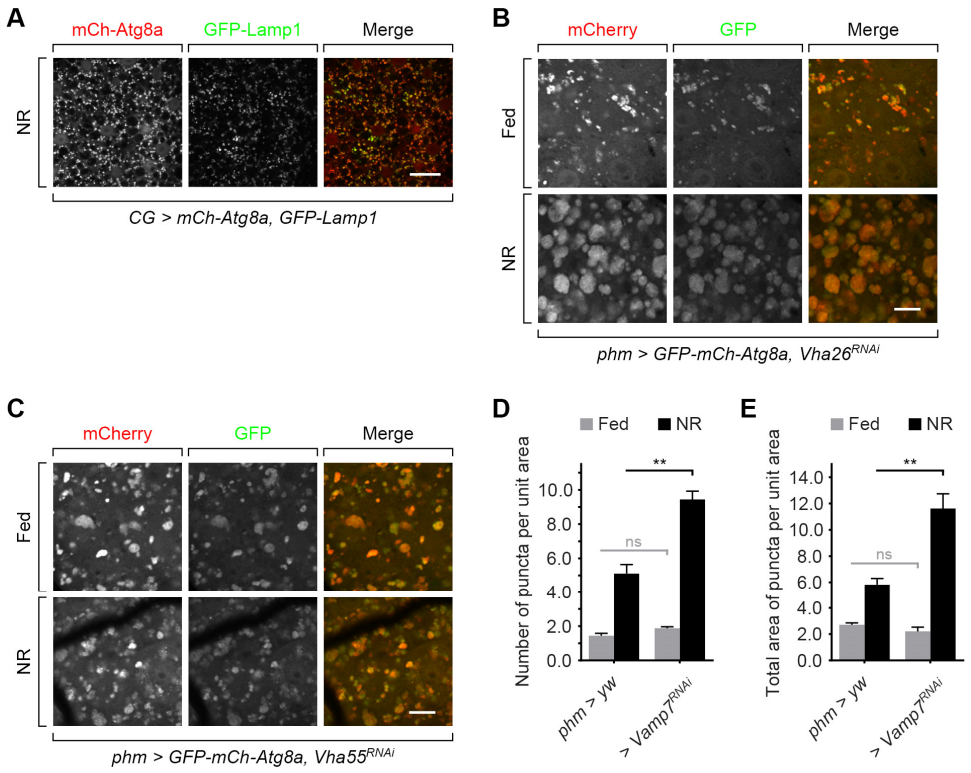

Figure S5. Autophagy affects cholesterol trafficking by interacting with endo/lysosomes. Related to Figure 6.

(A) Fluorescence microscopy images of fat body tissue expressing mCh-Atg8a and GFP-Lamp1. Scale bar, 50 μm. (B and C) Autophagy visualized by tandem tagged Atg8a in *phm>Vha26*^{RNAi} (B) and *phm>Vha55*^{RNAi} (C) PGs. Scale bar, 10 μm. (D and E) Quantification of number (D) and total area (E) of Atg8a positive puncta per unit cell area (100 μm^2) in control and *Vamp7* knockdown PGs.

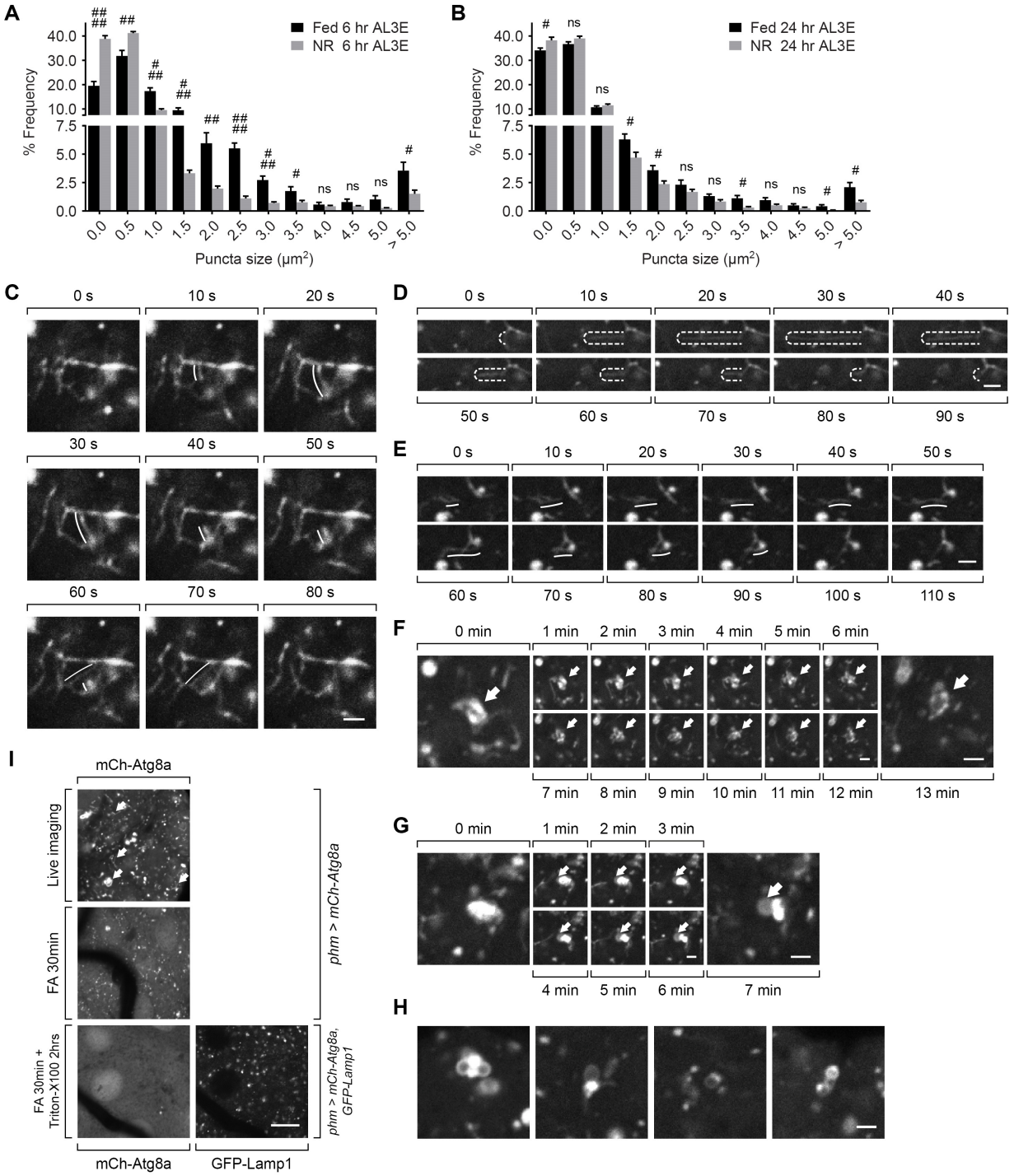
A
Fed 6 hr AL3E
NR 6 hr AL3E
% Frequency
Puncta size (μm²)
B
Fed 24 hr AL3E
NR 24 hr AL3E
% Frequency
Puncta size (μm²)
C
0 s
10 s
20 s
30 s
40 s
50 s
60 s
70 s
80 s
D
0 s
10 s
20 s
30 s
40 s
50 s
60 s
70 s
80 s
90 s
E
0 s
10 s
20 s
30 s
40 s
50 s
60 s
70 s
80 s
90 s
100 s
110 s
F
0 min
1 min
2 min
3 min
4 min
5 min
6 min
7 min
8 min
9 min
10 min
11 min
12 min
13 min
G
0 min
1 min
2 min
3 min
4 min
5 min
6 min
7 min
H
I
mCh-Atg8a
Live imaging
FA 30min
FA 30min + Triton-X100 2hrs
phm > mCh-Atg8a
phm > mCh-Atg8a, GFP-Lamp1
mCh-Atg8a
GFP-Lamp1

Figure S6. Autophagy in the PG is highly dynamic and exhibits additional non-conventional morphological features. Related to Figure 1.

(A and B) Frequency distribution of Atg8a-positive puncta size in 6 hrs (A) and 24 hrs AL3E (B) PGs. Mean ± SEM; p values by unpaired t-test (n=8; ns, not significant, #p<0.05, ##p<0.01, ###p<0.001, ####p<0.0001). (C) Time-lapse images showing an Atg8a-positive tubular network. A tubule formation event within the network is indicated by the solid lines. (D and E) Time-lapse images showing movement of Atg8a-positive tubular structures. A tubule protruding out from, and then retracting back to, a vesicle is outlined by the dash line (D). Another tubular structure moving toward and then fusing with a vesicle is indicated by the solid lines (E). (F) Time-lapse images showing fragmentation of a large Atg8a-positive vesicle. The morphological change is indicated by the arrows. (G) Time-lapse images showing formation of a ring-like structure (marked by arrows) beside an existing vesicle. (H) Additional static images of ring-like structures budded from existing vesicles. (C-H) Scale bar, 2 μm. (I) Autophagy in the PG visualized by confocal microscope under live imaging and after treatment by fixative and detergent. FA 30 mins, treatment by fixative (3.7% formaldehyde) for 30 mins. FA 30 mins + Triton X-100 2 hrs, treatment by detergent (0.1% Triton X-100) following FA fixation. White arrows show the tubule- and ring-like structures under live imaging. GFP-Lamp1 shows that lysosome structures are not sensitive to detergent treatment. Scale bar, 10 μm.

Supplemental Reference

S1. Chang, Y.Y., and Neufeld, T.P. (2009). An Atg1/Atg13 complex with multiple roles in TOR-mediated autophagy regulation. Mol. Biol. Cell *20*, 2004-2014.